

---

# AFM Study of Indirect Effect of Electric Discharge-Treated Steel on a Heme-Containing Enzyme

---

Ekaterina E. Vazhenkova , [Ivan D. Shumov](#) , [Vadim Yu. Tatur](#) , [Alexander N. Ableev](#) , [Andrey F. Kozlov](#) , [Natalia S. Bukharina](#) , [Ekaterina D. Nevedrova](#) , Angelina V. Vinogradova , Maria A. Agletdinova , [Andrei A. Lukyanitsa](#) , [Nina D. Ivanova](#) , [Alexander Yu. Dolgoborodov](#) , [Oleg F. Petrov](#) , Sergey V. Novikov , [Andrey N. Morozov](#) , [Anna V. Grudo](#) , [Alexander I. Archakov](#) , [Vadim S. Ziborov](#) , [Yuri D. Ivanov](#) \*

Posted Date: 1 May 2026

doi: 10.20944/preprints202604.2198.v1

Keywords: electric discharge; atomic force microscopy; peroxidase; cytochrome P450; enzyme aggregation; enzyme adsorption; knotted electromagnetic fields



Preprints.org is a free multidisciplinary platform providing preprint service that is dedicated to making early versions of research outputs permanently available and citable. Preprints posted at Preprints.org appear in Web of Science, Crossref, Google Scholar, Scilit, Europe PMC, OpenAlex.

Copyright: This open access article is published under a [Creative Commons CC BY 4.0 license](#), which permit the free download, distribution, and reuse, provided that the author and preprint are cited in any reuse.

Disclaimer/Publisher's Note: The statements, opinions, and data contained in all publications are solely those of the individual author(s) and contributor(s) and not of MDPI and/or the editor(s). MDPI and/or the editor(s) disclaim responsibility for any injury to people or property resulting from any ideas, methods, instructions, or products referred to in the content.

Article

# AFM Study of Indirect Effect of Electric Discharge-Treated Steel on a Heme-Containing Enzyme

Ekaterina E. Vazhenkova <sup>1</sup>, Ivan D. Shumov <sup>1,2</sup>, Vadim Yu. Tatur <sup>3</sup>, Alexander N. Ableev <sup>1</sup>,  
Andrey F. Kozlov <sup>1</sup>, Natalia S. Bukharina <sup>1</sup>, Ekaterina D. Nevedrova <sup>1</sup>, Angelina V. Vinogradova <sup>1</sup>,  
Maria A. Agletdinova <sup>1</sup>, Andrei A. Lukyanitsa <sup>3,4</sup>, Nina D. Ivanova <sup>3,5</sup>,  
Alexander Yu. Dolgoborodov <sup>2</sup>, Oleg F. Petrov <sup>2</sup>, Sergey V. Novikov <sup>6</sup>, Andrey N. Morozov <sup>7</sup>,  
Anna V. Grudo <sup>8</sup>, Alexander I. Archakov <sup>1</sup>, Vadim S. Ziborov <sup>1,2</sup> and Yuri D. Ivanov <sup>1,2,\*</sup>

<sup>1</sup> Laboratory of Nanobiotechnology, Institute of Biomedical Chemistry, 10, Pogodinskaya st.,  
Moscow 119121, Russia

<sup>2</sup> Joint Institute for High Temperatures of the Russian Academy of Sciences, 13 Bd.2, Izhorskaya st.,  
Moscow 125412, Russia

<sup>3</sup> Foundation of Perspective Technologies and Novations, 8 bld. 1, 2nd Ambulatory rd., Moscow 125315,  
Russia

<sup>4</sup> Faculty of Computational Mathematics and Cybernetics, Lomonosov Moscow State University, Leninskie  
Gory, 1, Moscow 119991, Russia

<sup>5</sup> Moscow State Academy of Veterinary Medicine and Biotechnology Named after Skryabin, 23, Academician  
Skryabin st., Moscow 109472, Russia

<sup>6</sup> Associate Printing-and-Publication Centre Technosphera, 16 Bd.2, Krasnoproletarskaya st., Moscow 127473,  
Russia

<sup>7</sup> Federal State Autonomous Educational Institution of Higher Education «Bauman Moscow State Technical  
University», 5 Bd. 1, 2nd Baumanskaya st., Moscow 105005, Russia

<sup>8</sup> Institute of Bioorganic Chemistry of the National Academy of Sciences of Belarus, 5/2, Academician  
Kuprevich St. 220084 Minsk, Republic of Belarus

\* Correspondence: yurii.ivanov.nata@gmail.com

## Abstract

Heme-containing enzymes play vital functions in living organisms, including humans. Here we demonstrate two indirect effects of (electric discharge)-treated stainless steel on a model enzyme — horseradish peroxidase (HRP). The first effect is the complete loss of the enzyme's adsorption after its incubation in grounded stainless steel chamber, which has been preliminarily subjected to electric discharge in air at atmospheric pressure. The second one is the formation of enzyme aggregates in the sample incubated in another grounded chamber two meters away from the discharge-treated one. At that, the HRP's enzymatic activity is found to be unaffected in the both cases. These effects may be explained by the occurrence of knotted electromagnetic fields (KEMF). By using high-speed atomic force microscopy (HS-AFM), we reveal the relatively high surface mobility of cytochromes P450cam and P450 102A1 (BM3), whose isoelectric point (pI) values are acidic; at that, thymidylate synthase (TYMS) with near-neutral pI adsorbs strongly. Thus, HRP is the best model object, since its basic pI provides quite strong adsorption on mica. Since (electric discharge)-processed materials have found applications in medicine, we expect that the effects discovered will be considered in future biomedical applications of (electric discharge)-based technologies.

**Keywords:** electric discharge; atomic force microscopy; peroxidase; cytochrome P450; enzyme aggregation; enzyme adsorption; knotted electromagnetic field

## 1. Introduction

Gas discharges occur upon passing of electric current through a gas at various gas pressures ranging from atmospheric one down to several Pascals [1–3]; at that, the gas turns into either partially or fully ionized state, which has been called plasma [1]. To date, both the gas discharge as a phenomenon and the plasma (produced from the initial plasma-forming gas) as a medium have found numerous technological applications. The applications of gas-discharge plasma include – but are not limited to - water purification [4,5], surface decontamination [6] and sterilization [7,8]. Gas discharges, in their turn, are applied, for instance, for precise machining of conductive materials (metals and alloys) [9], including steel [10,11]. Regarding the latter, the use of electric discharge machining (EDM) for fabrication of medical tools should be emphasized<sup>9,12</sup>. Technologies based on gas discharges have also found many other applications in medicine, including surface treatment of both inorganic and organic materials [13].

Interaction of an electric discharge with biological macromolecules can be either direct or indirect (Figure 1a) [14]. The direct interaction implies direct contact of the gas-discharge plasma with the biological macromolecules. In contrast, an interaction of discharge-processed materials with the biological macromolecules without their direct introduction into the discharge area represents the indirect interaction [15,16]. While direct effects of electric discharge on biological macromolecules were already reported [17,18], the indirect ones are poorly studied. Typical example of the latter is the dissolution of a sample in plasma-processed water [16].

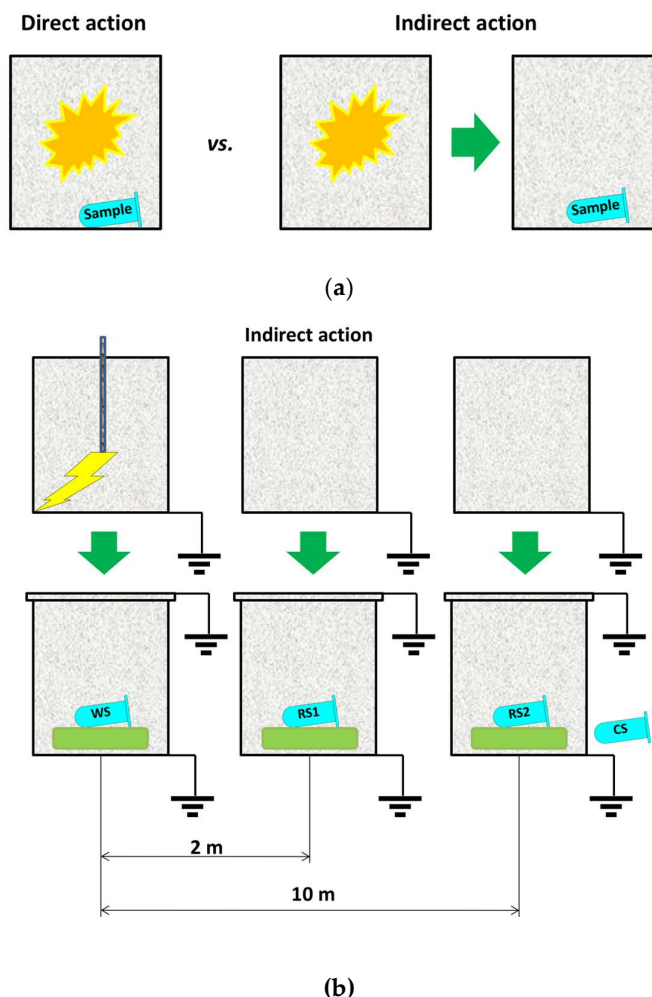


**Figure 1.** Schematic illustration of direct and indirect action of electric discharge on an enzyme sample (a), and implementation of the indirect action of electric discharge in our experiments (b, not to scale).

Direct effects of gas discharges and gas-discharge plasma on biomolecules, including enzymes, are well known [17,18], though research in this direction is actively continued. In contrast, as we are aware, indirect effects of (electric discharge)-processed solid materials on biomolecules are yet unknown. At that, electric discharges are used for processing of conductive materials (including steel [10,11] intended for medical applications [9,12], thus implying indirect interaction of electric discharge on biological tissues and macromolecules – including enzymes. The latter is what we consider herein.

Atomic force microscopy (AFM) was shown to be a useful approach to single-molecule imaging of heme-containing enzyme [19,20]. AFM allows one to reveal even minor effects of magnetic [21,22] and electromagnetic [23,24] fields on their physicochemical properties. Heme-containing enzymes catalyze many vital processes in living organisms. In general, high-valent iron-oxo heme proteins catalyze oxidation of various compounds by either molecular oxygen or hydrogen peroxide [25]. Namely, monooxygenases of cytochrome P450 superfamily play key roles in oxygenation of fatty acids and various xenobiotics by molecular oxygen [26,27]. Heme-containing peroxidases, in their turn, participate in oxidation of various compounds by hydrogen peroxide [28]. The key roles of the processes, catalyzed by heme-containing enzymes, determines the importance of studies concerning the influence of various external factors on the functioning of heme-containing enzymes. These factors include (though are not limited to) [29,30] electromagnetic fields, which may affect enzyme structure and functionality [23,31,32].

In order to justify the choice of HRP as a model enzyme in experiments on the investigation of indirect effects of (electric discharge)-treated stainless steel on heme-containing enzymes, we use the illustrative examples of enzymes with acidic and near-neutral isoelectric point (pI) values. The data obtained for HRP are compared with the effect caused by direct exposure of the enzyme to 10 nW/cm<sup>2</sup> knotted electromagnetic field (KEMF). The first effect of the discharge-processed steel is the complete loss of the enzyme's adsorbability after its incubation in grounded stainless steel container, which has been preliminarily subjected to electric discharge in air at atmospheric pressure. The second effect is the formation of enzyme aggregates in the sample incubated in another grounded container two meters away from the discharge-treated one. At that, the HRP's enzymatic activity is found to be unaffected in the both cases. Direct exposure to KEMF is shown to induce considerable aggregation of the enzyme, do not affecting its activity. These effects may be explained by the occurrence of KEMF [23]. Since (electric discharge)-processed materials find their application in medicine [13], we expect that the effects discovered herein will be considered in future biomedical applications of (electric discharge)-based technologies.

High-speed atomic force microscopy (HS-AFM) developed by Professor T. Ando et al. [33,34] represents a powerful tool, which allows one to visualize dynamic processes in enzyme systems (including heme-containing enzymes) [35] with high time resolution. By HS-AFM, Takeda et al. demonstrated real-time visualization of adsorption of cytochrome C [35]. Continuous successful work on improving the spatial resolution and reducing noise of HS-AFM imaging is being performed, as was quite recently demonstrated by Sato et al. [36]. Herein, by HS-AFM, we experimentally demonstrate high surface mobility of two different cytochromes of P450 superfamily – P450cam and cytochrome P450 102A1 (P450 BM3) – in buffer with physiological pH 7.4; the isoelectric point (pI) values of these enzymes are acidic [37,38]. This is in contrast to the case with thymidylate synthase (TYMS), whose pI is near-neutral [39]. This is how we motivate the choice of horseradish peroxidase (HRP) with basic pI as a model enzyme in the investigation of effect of electric discharge-treated steel on a heme-containing enzyme in subsequent experiments reported herein.

## 2. Results

Firstly, cytochromes P450cam and P450 BM3 were studied by HS-AFM. Figure 2 displays HS-AFM images clipped from videos recorded by HS-AFM scanning of mica with adsorbed enzymes.

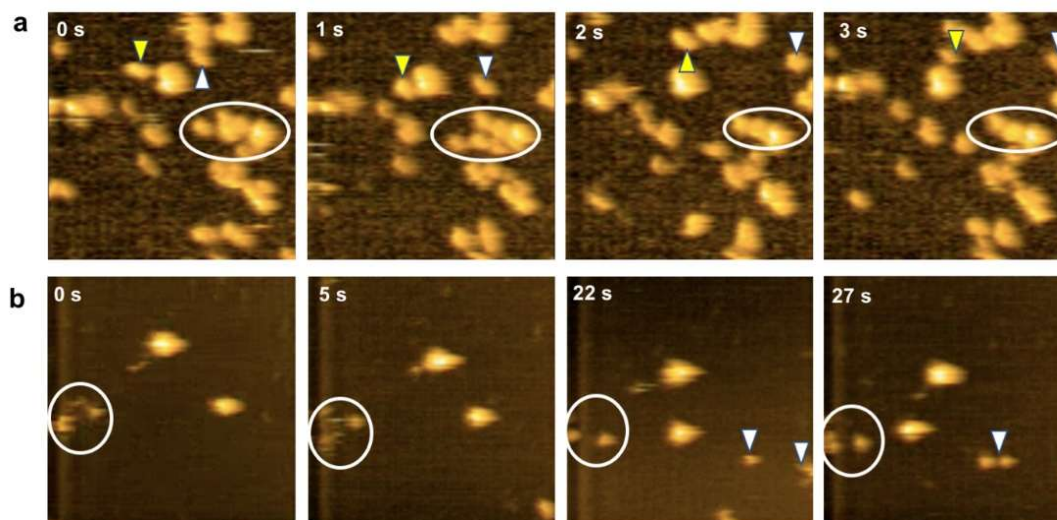


**Figure 2.** HS-AFM observation of cytochrome P450cam (a) and cytochrome P450 BM3 (b) adsorbed on mica. In a, yellow and white triangles point at different P450cam molecules, which move rapidly along the mica surface and sometimes form instable aggregates with other stronger adsorbed molecules. Circle marks instable enzyme aggregate in the right area of the images. In b, white triangles point at different P450 BM3 molecules, which occur in the images owing to their fast moving along mica surface. A group of moving P450 BM3 molecules is circled in the left area of the images. The images are clipped from videos recorded at 100 ms per frame and 100 nm × 100 nm frame size.

For the both cytochromes, the images clipped from successfully captured HS-AFM videos and shown in Figure 2 indicate the presence of many weakly adsorbed enzyme molecules, which form unstable aggregates on the mica surface at physiological pH, thus hindering correct determination of the enzyme aggregation state under experimental conditions (see Supplementary videos S1 and S2 for cytochrome P450cam and P450 BM3, respectively).

The high mobility of cytochromes P450cam and P450 BM3 on mica under our experimental conditions can be explained by the fact that at pH 7.4, the molecules of these enzymes bear a negative net charge. Indeed, the experimentally determined pI value of cytochrome P450cam is 4.55 [37]; reductase domain of P450 BM3 has a pI near 5 [38], while theoretical pI of the whole enzyme is ~5.34. The surface of bare mica, in its turn, also was reported to bear a pH-independent negative charge, whose value is determined by the mineral's crystalline lattice and is equal to  $-2.1e$  per  $\text{nm}^2$ ; in addition, dissociation of potassium ions on mica surface can also make a contribution to its charging [40]. These facts imply electrostatic repulsion between the mica surface and the P450cam and P450 BM3 enzyme molecules at near-neutral pH. Videos recorded by HS-AFM, however, show that molecules of the both enzymes do approach the mica surface and form aggregates on it, though the adsorption is quite weak, and the aggregates are unstable. These results can be well explained by heterogeneous properties of enzyme molecules' surface [41,42] and the so-called cooperative effect discussed by Luo and Andrade [42]. Namely, an enzyme can adsorb onto mica even if pH exceeds the enzyme's pI owing to the presence of local positively charged areas on the surface of enzyme molecules [42]. And this is what we observe in our HS-AFM experiments with the both cytochromes.

The case with TYMS shown in Figure 3 is in contrast with the situation observed with cytochromes and discussed above.

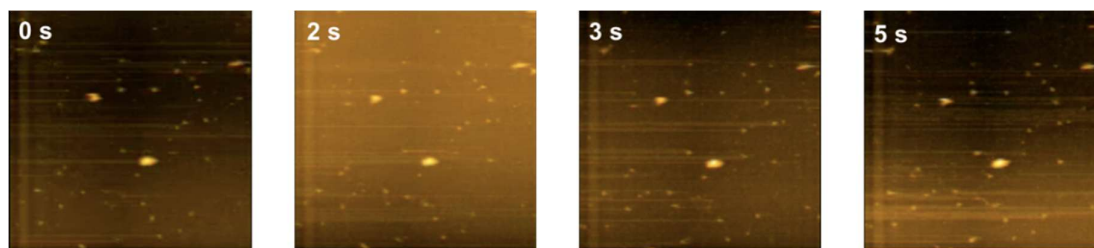


**Figure 3.** HS-AFM observation of TYMS adsorbed on mica. The images are clipped from video recorded at 520 ms per frame and 400 nm × 400 nm frame size.

Indeed, TYMS molecules virtually do not move after their adsorption on mica (see Figure 3 and Supplementary Video S3). TYMS was reported to have near-neutral pI of 6.7 [39], and this explains its strong adsorption observed in buffer with pH of 7.4.

Accordingly, tighter adsorption of an enzyme of interest is strongly required in order to correctly determine alterations of its aggregation state under an external action. In this respect, alteration of acidity of the medium is one of the ways towards promoting the enzyme adsorption: namely, the use of moderately acidic acetate buffer often favours the electrostatically driven enzyme adsorption [43]. In our study, we aim at maintaining the pH at near-physiological values [23]. In this case, proper selection of the model enzyme is required.

The results described above confirm the right choice of HRP as a model in further experiments. The pI of HRP-C isozyme makes up 8.9 [44]. This value is much higher than those of the both cytochromes studied by HS-AFM and provides quite strong adsorption on mica, allowing us to correctly determine the enzyme's aggregation state on mica by conventional AFM. In order to reveal yet unknown effects of stainless steel, subjected to electric discharge in air at atmospheric pressure, on HRP, we employed the well-established method of combined use of conventional atomic force microscopy and spectrophotometry [23]. The discharge was generated in a completely grounded metal volume (Figure 1b) with a RESINBLOK 2000 20 kV, 50 Hz AC high voltage generator (F.a.r.t. S.p.A.; Italy). The discharge was generated in the grounded stainless steel chamber for 15 minutes, and then the chamber was cooled down to room temperature in order to avoid heating of the enzyme sample. Then, an Eppendorf-type test tube with 1 mL sample of 0.1  $\mu$ M solution of HRP was placed into the chamber onto a foamed polyurethane gasket, and the chamber was covered with a grounded 2-mm-thick steel cap. In this way, the discharge chamber represented a ground-shield for the working enzyme sample (WS), which was incubated therein for 40 minutes. At the same time, two reference enzyme samples were incubated in similar fully grounded steel chambers, which were not subjected to the discharge. One of these chambers with reference enzyme sample RS1 was placed two meters away from the one subjected to the discharge, while the other one with reference enzyme sample RS2 was placed a separate room ten meters away from the experimental setup. The control enzyme sample CS was also incubated in the same room as the RS2 sample. All the four HRP samples were then analyzed by AFM and spectrophotometry employing the technique developed and described in our previous studies [23,24,29]. And the results of our analysis were quite surprising (Figures 4 and 5a).

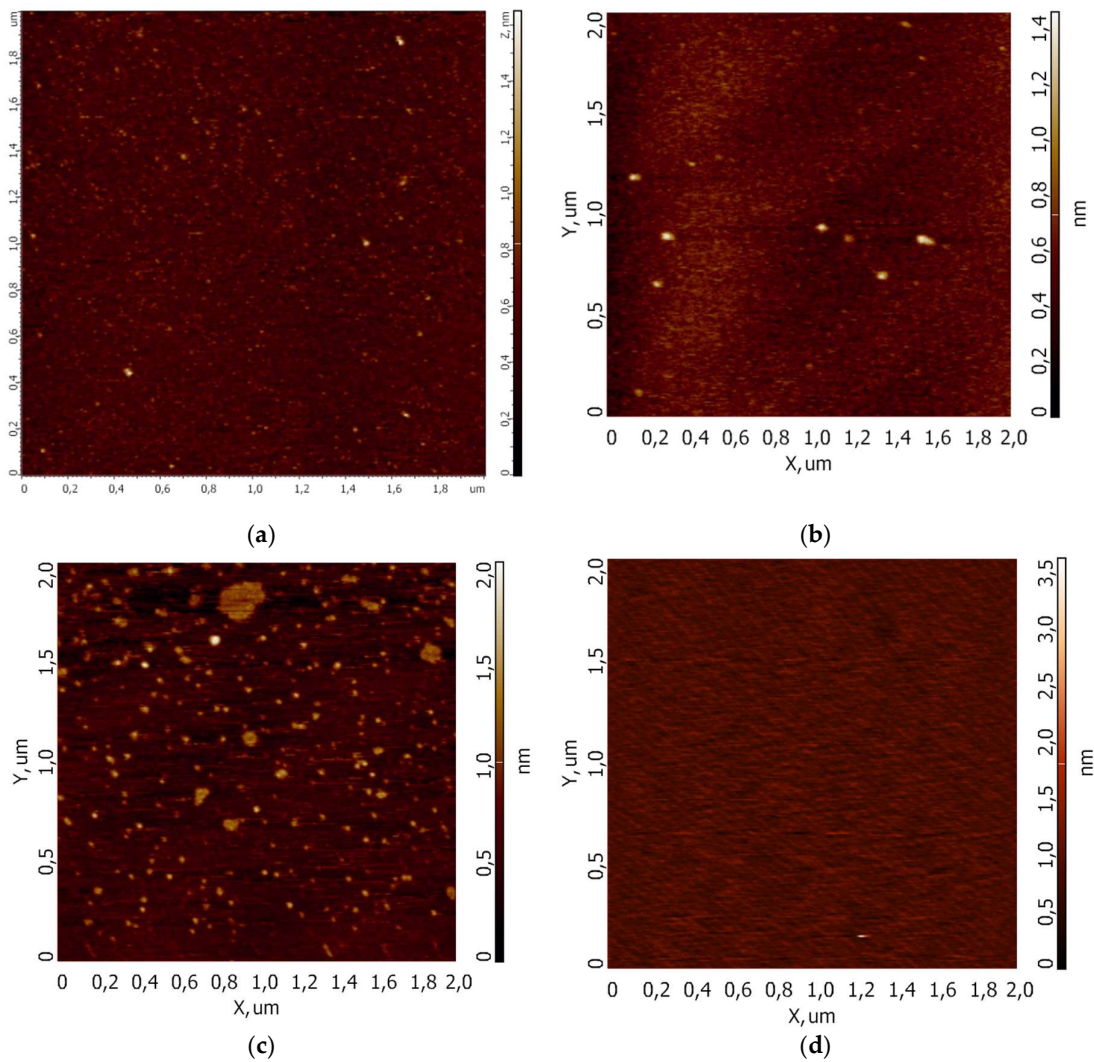


**Figure 4.** Typical AFM images of mica substrate surface obtained in AFM analysis of HRP in either of the following samples: control sample CS incubated 10 m away from the experimental setup (a), reference sample 2 RS2 incubated setup in ground-shielded chamber 10 m away from the experimental setup (b), reference sample 1 RS1 incubated in the ground-shielded chamber 2 m away from the experimental setup (c), and working sample WS incubated in ground-shielded chamber after its treatment to electric discharge (d). The size of all images is  $2 \mu\text{m} \times 2 \mu\text{m}$ .

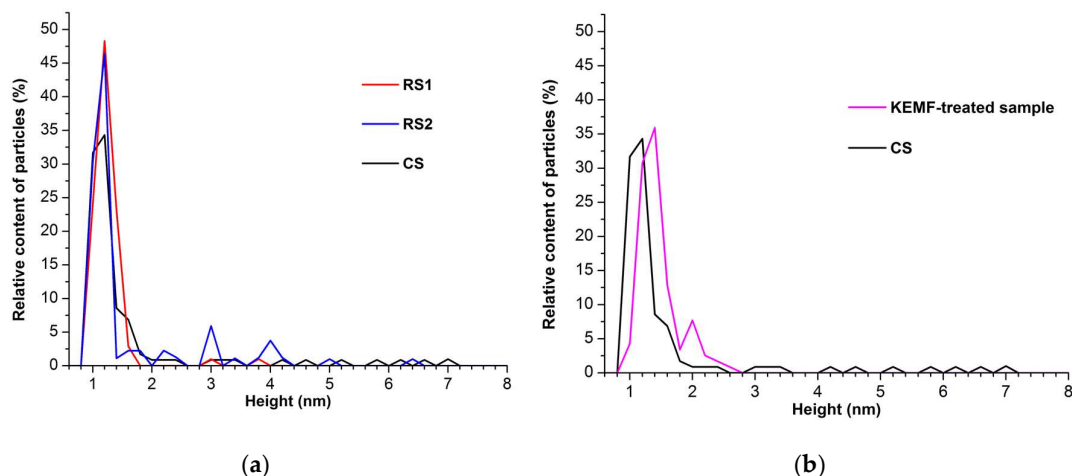


**Figure 5.** Distributions of HRP particles, adsorbed on mica, with height. (a) Distributions obtained for samples studied in experiments with electric discharge. Line colour indicates curves obtained for the control sample CS incubated 10 m away from the experimental setup (black), reference sample 2 RS2 incubated setup in ground-shielded chamber 10 m away from the experimental setup (blue), and reference sample 1 RS1 incubated in the ground-shielded chamber 2 m away from the experimental setup (red). No particles adsorbed from the working sample WS incubated in ground-shielded chamber after its treatment to electric discharge. (b) Distributions obtained for samples studied in experiments with KEMF. (b) Line colour indicates distributions obtained for the control sample CS incubated 10 m away from the experimental setup (black), and for the sample irradiated in 10 nW/cm<sup>2</sup> KEMF at a 0.64 m distance from the emitter (magenta).

In the case of both the control sample CS and the reference sample RS2, which were placed ten meters away from the experimental setup, the enzyme adsorbed onto mica in the form of compact objects, whose height typically did not exceed the 1.2 nm value (Figure 4a,b; Figure 5a, black and blue curves). As was determined previously, these objects represent monomeric HRP adsorbed on mica [9]. The content of oligomeric HRP in the both samples, incubated at the 10 m distance from the setup, was negligible. In contrast, the RS1 sample incubated at shorter (2 m) distance from the setup contained considerable (23%) amount of oligomeric HRP particles of 1.4 nm height (Figure 5a, red curve). Typical AFM image of HRP, adsorbed on mica from the RS1 sample, clearly indicates the presence of extended objects on the mica substrate – in contrast to the samples incubated at longer (10 m) distance from the setup (Figure 4c). These extended objects correspond to large high-order HRP aggregates. Moreover, the results of the analysis of the working sample WS were quite amazing, since no enzyme at all was detected on the mica surface: the mica surface was quite flat (Figure 4d). We should emphasize that the enzymatic activity of HRP against ABTS substrate in all samples studied was approximately equal (Figure 6).

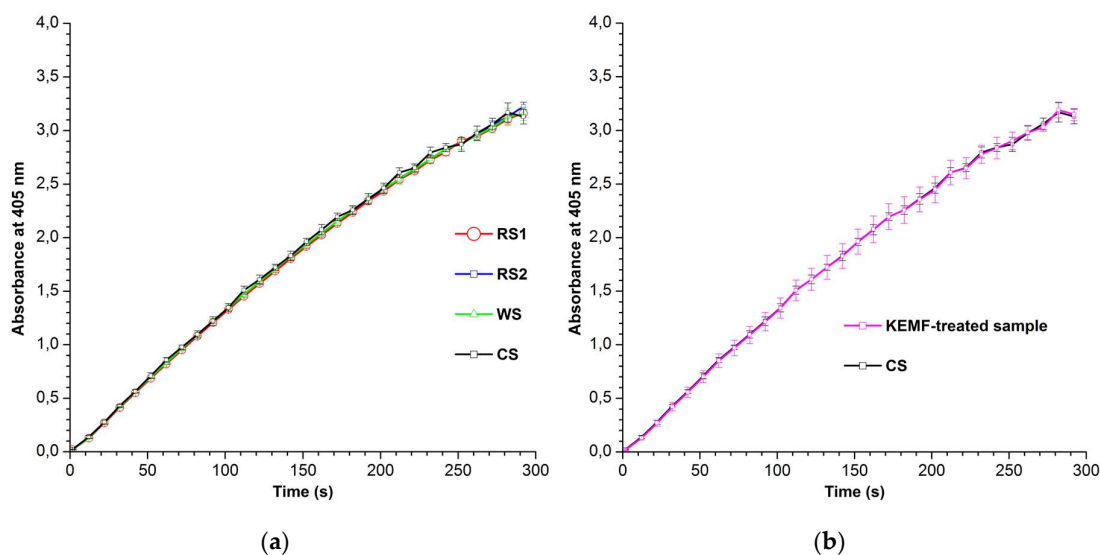


**Figure 6.** Kinetic curves obtained upon estimation of enzymatic activity of HRP in the samples studied against ABTS. (a) Curves obtained for samples studied in experiments with electric discharge. Line colour indicates curve obtained for the control sample CS incubated 10 m away from the experimental setup (black), reference sample 2 RS2 incubated setup in ground-shielded chamber 10 m away from the experimental setup (blue), reference sample 1 RS1 incubated in the ground-shielded chamber 2 m away from the experimental setup (red), and working sample WS incubated in ground-shielded chamber after its treatment to electric discharge (green). (b) Curves obtained for samples studied in experiments with KEMF. Line colour indicates curve obtained for the control sample CS incubated 10 m away from the experimental setup (black), and for the sample irradiated in 10 nW/cm<sup>2</sup> KEMF at a 0.64 m distance from the emitter (magenta).

### 3. Discussion

The results of our experiments can be explained in the following way. Action of an electric discharge on metal materials, including steels, induces occurrence of stress [10,11,45,46], which persists after the discharge action is finished. The well-known cause of discharge-induced stress is uneven heating/cooling during the electric discharge. Here, we should emphasize the relationship between thermal effects of electric discharge action on metals and the stress: while local heating effect is utilized in EDM [10] the reverse process was also discussed [47]. At atomic level, the internal stress in metal represents a distortion of its lattice; the stress also changes the metal's microstructure [48]. As a result, mechanical energy is accumulated in the microstructure of the metal in the form of elastic deformation. Furthermore, electric discharges are accompanied by electromagnetic emission. At that, Song et al. emphasize that external electric or magnetic fields (which are known to be interconnected) can transfer high energy directly to the electronic scale of metal materials, changing spin, energy level arrangement and trajectory of electrons in the metal [48]. In other words, the action of electric discharge on a metal can induce transfer of its atoms to their excited states. And the reverse process of transfer of atoms from their excited states to the unexcited one is known to be accompanied by electromagnetic radiation. The action of the latter on the enzyme, in its turn, can be the very cause of the observed disappearance in the enzyme's adsorbability. Indeed, HRP is known to be quite sensitive to electromagnetic radiation, though its effects on the enzyme can sometimes be revealed by only single-molecule investigation [23,24].

In the experiments reported, we observed the aggregation of the enzyme in the RS1 sample incubated at the 2 m distance from the experimental setup, despite the sample was ground-shielded. This phenomenon can be explained by the specific topology of KEMF [49,50] emitted by the discharge-treated steel chamber located two meters away. Unlike transverse electromagnetic fields, knotted ones are able to pass through metallic shields, even if the latter are grounded [50]. Previously, we demonstrated that knotted electromagnetic field (KEMF) of even very low (1 pW/cm<sup>2</sup>) power

density induces aggregation of HRP incubated at a comparable (0.64 m) distance from the emitter<sup>23</sup>. In order to prove our explanation, herein, we repeated our experiments with KEMF at ten thousand times higher (10 nW/cm<sup>2</sup>) power density. Upon AFM analysis of the enzyme sample exposed to KEMF, considerable amount of 2-nm-high HRP aggregates has been revealed (Figure 5b, magenta curve) in comparison with the control enzyme sample incubated ten meters away from the KEMF emitter (dotted black curve). At that, the maximum of the respective distributions of mica-adsorbed HRP particles with height shifted to the 1.4 nm value, indicating aggregation of the enzyme in KEMF-treated sample. And similar to both the recent experiments with discharge-processed steel and the previously reported experiments with KEMF at lower 1 pW/cm<sup>2</sup> power density, KEMF was found to have no effect on the HRP's enzymatic activity against ABTS (Figure 6b) [23]. These results and the fact that the RS1 sample was completely ground-shielded (Figure 1b) confirm our explanation of the effect of the discharge-processes steel on the enzyme placed at a distance of two meters.

The observed changes in adsorbability of HRP on mica can be explained by the alterations in the surface structure of enzyme globules [29]. These alterations affect all of the following interactions: enzyme-enzyme, enzyme-solvent and enzyme-(AFM substrate surface) [29]. These interactions are, to a great extent, determined by the structure of hydration shell surrounding the HRP enzyme globule [51,52]. It is to be emphasized that only hydration shell of the enzyme has undergone structure alterations in our experiments, while its active site remained unaffected. This is how we explain the results obtained in our experiments with HRP.

One should emphasize that action of magnetic field can induce more dramatic alterations in the structure of heme-containing enzymes, causing changes in enzymatic activity<sup>32</sup>. In our experiments with HRP, no change in enzymatic activity is revealed, supporting our conclusion that only outer hydration shell of the enzyme globules is affected. The latter obviously influences the enzyme-enzyme, enzyme-(AFM substrate surface) and enzyme-solvent interactions, while not affecting the active site and the conformation of the peptide chains. The high stability of the HRP's spatial structure can be explained by high carbohydrate content, which makes up 18 to 27% [44]. The situation with other heme-containing enzymes such as cytochromes P450cam and P450 BM3 may be quite different, but further work on careful selection of experimental conditions is required owing to high surface mobility of these enzymes at physiological pH. This is the subject of future studies, and herein we just demonstrate the great potential of HS-AFM in the revelation of surface mobility of heme-containing enzymes with acidic pI values. Since the surface mobility is directly determined by enzyme-(AFM substrate surface) interactions, HS-AFM represents an excellent tool for studies of effects of electromagnetic fields on heme-containing enzymes.

The growing application of electric discharge-processed and plasma-processed materials for medical applications [9,12,13] determines the great importance of effects discovered herein for future development of applications of (electric discharge)-based technologies in biomedicine. In this connection, a wide range of applications of HRP in biotechnology and medicine should be mentioned [53]. Regarding its biomedical applications, we should emphasize the wide use of HRP as a reporter enzyme in diagnostic systems<sup>53</sup> — including nanowire-based ones [54], which are known to have a great potential in highly sensitive revelation of various disease biomarkers (such as proteins — including enzymes — and nucleic acids) in humans [55,56]. The high sensitivity of nanowire and nanoribbon-based systems, which reaches just several charges per one sensor element, is achieved thanks to the very high surface-to-volume ratio of nanowire and nanoribbon sensor elements [57]. This fact emphasizes the importance of the in-deep studies of indirect effects of materials, which were subjected to electric discharge action and are intended for biomedical applications, on heme-containing enzymes [9,12]. Our experiments demonstrate promising application of HS-AFM in this area. However, our HS-AFM experiments with cytochromes of P450 superfamily reveal the strong need for further research in this direction in order to carefully determine optimal experimental conditions for each enzyme of interest.

## 4. Materials and Methods

*Enzymes.* Peroxidase from horseradish (HRP-C; Cat. # P6782) and its substrate, diammonium 2,2'-azino-bis(3-ethylbenzothiazoline-6-sulfonate) (ABTS), were purchased from Sigma (St. Louis, MA, USA).

Cytochrome P450cam was kindly donated by Professor G. Hui Bon Hua (French Institute of Health and Medical Research, France). The initial enzyme sample was received in the form of 1.8 mM stock solution in 100 mM potassium phosphate buffer (pH 7.0), which was stored at minus 80°C.

Wild-type cytochrome CYP102A1 was kindly donated by Professor A.W. Munro (University of Manchester, UK); the enzyme was expressed and prepared as described by Neeli et al.<sup>27</sup>. This enzyme was also expressed by Dr. Anna W. Grudo. The initial enzyme samples were received in the form of 40 µM stock solution. Aliquots of the stock solutions were stored at -80°C until their use in experiments.

Thymidylate synthase (TYMS) was purchased from Novus Biologicals (USA; Cat. #NBP1-30310; 1-133 aa; 36 kDa molecular weight). An aliquot of the original preparation was diluted by Dulbecco's modified phosphate buffered saline to the desired concentration.

*Chemicals.* Disodium hydrogen orthophosphate (Na<sub>2</sub>HPO<sub>4</sub>, analytical grade), citric acid (of highest purity, "of reference purity") and hydrogen peroxide (H<sub>2</sub>O<sub>2</sub>, analytical grade) were purchased from Reakhim (Moscow, Russia). Dulbecco's modified phosphate buffered saline (PBS-D; pH 7.4) was prepared by dissolving the salt premix purchased from Pierce (USA) in water. All aqueous solutions used in our experiments were prepared using ultrapure deionized water of 18.2 MΩ×cm resistivity, purified with a Simplicity UV system (Millipore, Molsheim, France). The solutions used in the AFM and HS-AFM experiments were additionally checked by AFM in order to confirm absence of particles with ≥1 nm size in them.

*HS-AFM experiments.* Either of the enzymes (cytochrome P450cam, P450 BM3, or TYMS) was adsorbed onto a freshly cleaved mica substrates by direct surface adsorption [58]. A 2-µL droplet of a 0.25 µM enzyme solution in 10 mM Dulbecco's modified phosphate buffered saline (PBS-D; pH 7.4) was dispensed on a mica substrate and incubated thereon for three minutes, and then washed off with ultrapure water. The so-prepared substrate was placed into the measuring cell of a RIBM high-speed atomic force microscope (manufactured by Professor T. Ando's scientific group in Japan and installed in IBMC, Moscow, Russia) containing 2.5 mM PBS-D (pH 7.4). HS-AFM scanning was performed in liquid using gold-coated NanoWorld probes (curvature radius <10 nm; probe beam length 2.5 µm; cantilever resonant frequency in air and liquid ~1.5 MHz and 0.9 MHz, respectively; spring constant ~0.6 N/m).

*Conventional AFM experiments.* In experiments with HRP, we used 0.1 µM solution of the enzyme in 2 mM PBS-D prepared by sequential tenfold dilution of its 10 µM stock solution. The latter was prepared by dissolution of a certain amount of the lyophilized enzyme preparation in 2 mM PBS-D. At each dilution step, the solution was kept in a Thermomixer Comfort shaker (Eppendorf, Germany) for 0.5 hour at 600 rpm and 23°C. The PBS-D buffer was prepared by dissolution of salt premix, purchased from Pierce (USA), in water. All solutions used in all experiments reported were prepared with ultrapure deionized (18.2 MΩ × cm) water obtained by purification of distilled water with a Simplicity UV system (Millipore, Molsheim, France).

*Experimental setup and experiments with electric discharge.* The high-voltage discharge was generated using a RESINBLOK 2000 high-voltage pulse generator (F.a.r.t. S.p.A.; Italy), which generates 20 kV, 50 Hz AC voltage. One of the generator's output contacts was connected to an electrode made of high purity electrical copper (electrode dimensions: length 180 mm, diameter 1.2 mm). The second output contact of the generator was connected to the bottom of a grounded stainless steel chamber (chamber dimensions: diameter 58 mm, height 72 mm, wall thickness 2 mm, floor thickness 3 mm; chamber material: AISI 304 stainless steel). The copper electrode was fixed in a textolite holder. The connection of the generator to the discharge chamber is schematically shown in Figure 7.

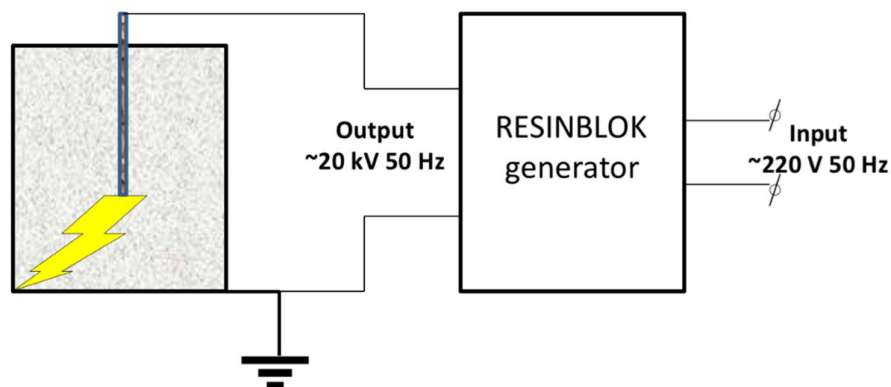


**Figure 7.** Schematic representation of connection of the generator to the discharge chamber.

In the experiments, 20 kV, 50 Hz AC voltage was supplied to the generator's output contacts, and the copper electrode was lowered into the center of the chamber until stable arc discharge was obtained between the electrode and the chamber surface. The discharge was allowed to pass through air at atmospheric pressure for four minutes. Then, the generator was powered off, and the camera was allowed to cool down to room temperature (23°C) for one minute. The temperature of the camera walls was controlled with a FY-10 thermocouple-based digital thermometer. The discharge treatment and camera cooling cycles were repeated three times. After the third cycle, a polyurethane foam gasket was laid into the camera, and a 1.5-mL Eppendorf type polypropylene test tube containing one milliliter of 0.1  $\mu\text{M}$  enzyme solution was laid onto the gasket. The inner space of the chamber was ground-shielded by covering the chamber with a grounded steel disc (disc dimensions: diameter 100 mm, thickness 2 mm; disc material: St-3 carbon steel). The WS working enzyme sample was kept in this chamber for 40 min. At the same time, test tubes with the RS1 and RS2 reference samples were put into exactly the same grounded chambers, which were not subjected to the discharge, and were placed two and ten meters away from the discharge-treated one. Tube with the control enzyme sample was kept outside the grounded chamber ten meters away from the experimental setup.

*Experimental setup and experiments with KEMF.* Detailed description of the experimental setup employed for irradiation of enzyme samples in KEMF was given in our pioneer paper [23]. Briefly, the setup contained an emitter antenna representing a five-leafed wire knot fixed on a central rod. The latter was connected to a half-wave vibrator with balancing and matching U-knee using a 50- $\Omega$  cable [9]. The KEMF parameters were set with a USB-TG44A Tracking Generator (Signal Hound, USA), and the radiation power was controlled with a USB-SA44B Spectrum Analyzer (Signal Hound, USA). Under the experimental conditions, no heating of the enzyme samples was observed, as was controlled with a FY-10 thermocouple-based digital thermometer. In comparison with the previously described experiments [23], the only difference was the KEMF power density, which amounted to 10 nW/cm<sup>2</sup> in our experiments reported herein – that is, ten thousand times higher than the 1 pW/cm<sup>2</sup> value in our pioneer work [23]. The distance between the emitter antenna and the test tube with the enzyme samples was 0.64 m, i.e., comparable to the 2 m value between the electric discharge-treated chamber and the chamber with the RS1 sample.

*Analysis of the enzyme samples.* All the enzyme samples treated in the experiments described above were studied employing a combined AFM and spectrophotometry analysis technique described in our previous papers<sup>23,24,29</sup>. Briefly, for AFM analysis, AFM substrates were prepared by direct surface adsorption<sup>58</sup> of HRP from either of the HRP samples onto bare mica. For each enzyme sample studied, a 7 mm  $\times$  15 mm mica substrate was immersed in an Eppendorf-type test tube containing 0.8 mL of the studied enzyme solution, and incubated therein for ten minutes in a Thermomixer Comfort shaker (Eppendorf, Germany) at 600 rpm and 23°C, then rinsed with ultrapure water and dried in air.<sup>23</sup> The mica substrates were scanned with a Prima atomic force

microscope (NT-MDT, Zelenograd, Russia) equipped with with NSG10 cantilevers (“TipsNano”, Zelenograd, Russia; from 140 to 390 kHz resonant frequency, from 3.1 to 37.6 N/m force constant, tip curvature radius 10 nm). The microscope was calibrated by height using a TGZ1 calibration grating (NT-MDT, Zelenograd, Russia; step height  $21.4 \pm 1.5$  nm). AFM operation, obtaining and treatment of the AFM images, and exporting the resulting data in ASCII format were performed with a standard NOVA Px software (NT-MDT, Moscow, Zelenograd, Russia) supplied with the microscope. The number of the visualized particles in the obtained AFM images was calculated automatically using an AFM data processing software custom-developed in IBMC (Rospatent registration no. 2010613458). Based on the so-obtained AFM data, distributions of the enzyme particles, adsorbed on mica, with height were calculated and plotted as described in our pioneer work [23]. The number of  $2 \mu\text{m} \times 2 \mu\text{m}$  frames obtained for each substrate was  $\geq 10$ .

**Spectrophotometry.** In parallel with the AFM analysis, spectrophotometry analysis of the enzyme samples was being performed [23,24,29]. Briefly, the activity of the enzyme against ABTS was estimated using an assay developed by Sanders et al. [59] Absorbance of a reaction solution containing the enzyme, ABTS and  $\text{H}_2\text{O}_2$  at 1 nM, 0.3 mM and 2.5 mM concentrations, respectively, in phosphate-citrate buffer (51 mM  $\text{Na}_2\text{HPO}_4$ , 24 mM citric acid, pH 5.0) [59] was monitored with an Agilent 8453 spectrophotometer (Agilent Deutschland GmbH, Waldbronn, Germany) in 1-cm-long quartz cell for five minutes at  $23^\circ\text{C}$ . The volume of 0.1  $\mu\text{M}$  enzyme solution used in each spectrophotometry measurement was 30  $\mu\text{L}$ . At least three independent measurements were performed for each sample studied. Statistic calculations were performed as described elsewhere [60].

**Supplementary Materials:** The following supporting information can be downloaded at the website of this paper posted on Preprints.org: Supplementary Video S1: HS-AFM observation of cytochrome P450cam; Supplementary Video S2: HS-AFM observation of cytochrome P450 BM3; Supplementary Video S3: HS-AFM observation of TYMS.

**Author Contributions:** Conceptualization, Y.D.I., V.Y.T. and A.I.A.; methodology, Y.D.I. and V.Y.T.; software, A.A.L.; validation, A.Y.D., O.F.P. and A.N.M.; formal analysis, N.D.I. and S.V.N.; investigation, E.E.V., I.D.S., V.Y.T., A.N.A., A.F.K., N.S.B., E.D.N., A.V.V., M.A.A., and V.S.Z.; resources, V.Y.T., A.Y.D., O.F.P. and A.N.M.; data curation, I.D.S., E.E.V. and S.V.N.; writing—original draft preparation, I.D.S. and Y.D.I.; writing—review and editing, I.D.S. and Y.D.I.; visualization, I.D.S. and N.S.B.; supervision, A.I.A.; project administration, Y.D.I.; funding acquisition, A.I.A. All authors have read and agreed to the published version of the manuscript.

**Funding:** The AFM and HS-AFM measurements were performed within the framework of the Program for Basic Research in the Russian Federation for a long-term period (2021-2030) (No. 122030100168-2). The spectrophotometry measurements, the experiments with the gas discharge setup, and the experimental work on the preparation and surface modification of AFM chips was supported by the Ministry of Science and Higher Education of the Russian Federation (State Assignment No. 075-00270-26-00).

**Institutional Review Board Statement:** Not applicable.

**Informed Consent Statement:** Not applicable.

**Data Availability Statement:** Data are provided within this paper and/or Supplementary Materials. Additional data underlying the research can be obtained from the corresponding authors upon reasonable request.

**Acknowledgments:** The authors are grateful to Dr. Pavel A. Frantsuzov for his kind assistance in experiments with cytochrome P450cam. The authors also thank Professor Andrew W. Munro (Institute of Manchester, UK) for kind donation of cytochrome P450 BM3 enzyme. The authors feel indebted to Dr. Gaston Hui Bon Hoa (deceased on 26 July 2020) for kind donation of cytochrome P450cam enzyme.

**Conflicts of Interest:** The authors declare no conflicts of interest.

## References

1. Bogaerts, A.; Neyts, E.; Gijbels, R.; van der Mullen, J. Gas discharge plasmas and their applications. *Spectrochim Acta Part B* **2002**, *57*, 609–658. [https://doi.org/10.1016/S0584-8547\(01\)00406-2](https://doi.org/10.1016/S0584-8547(01)00406-2).
2. Zhironov, A.V.; Belkin, P.N.; Kusmanov, S.A.; Shadrin, S.Yu. Distinctive features of electric current passing through vapour gaseous envelope in anodic plasma electrolytic processes. *J Phys: Conf Ser* **2020**, *1713*, 012049. <https://doi.org/10.1088/1742-6596/1713/1/012049>.
3. Shumova, V.V.; Polyakov, D.N.; Vasilyak, L.M. Neon dc glow discharge at cryogenic cooling: experiment and simulation. *J. Phys. D: Appl. Phys.* **2017**, *50*, 405202. <https://doi.org/10.1088/1361-6463/aa8292>.
4. Vishnyakov, V.I. Pulsed high-voltage electrical discharges in water: The resource for hydrogen production and water purification. *Int J Hydrogen Energy* **2022**, *47* (25), 12500-12505. <https://doi.org/10.1016/j.ijhydene.2022.02.015>.
5. Qasim, M.; Rafique, M.S.; Naz, R. Water purification by ozone generator employing non-thermal plasma. *Mater Chem Phys* **2022**, *291*, 126442. <https://doi.org/10.1016/j.matchemphys.2022.126442>.
6. Li, Z.; Li, Y.; Cao, P.; Zhao, H. Surface Decontamination of Chemical Agent Surrogates Using an Atmospheric Pressure Air Flow Plasma Jet. *Plasma Sci Tech* **2013**, *15* (7), 696. <https://doi.org/10.1088/1009-0630/15/7/17>.
7. Ito, M.; Hashizume, H.; Oh, J.-S.; Ishikawa, K.; Ohta, T.; Hori, M. Inactivation mechanism of fungal spores through oxygen radicals in atmospheric-pressure plasma. *Jpn J Appl Phys* **2021**, *60*, 01050. <https://doi.org/10.35848/1347-4065/abcbd1>.
8. Pei, X.; Liu, J.; Xian, Y.; Lu, X. A battery-operated atmospheric-pressure plasma wand for biomedical applications. *J. Phys. D: Appl. Phys.* **2014**, *47*, 145204. <https://doi.org/10.1088/0022-3727/47/14/145204>.
9. Abbas, N.M.; Solomon, D.G.; Bahari Md.A. A review on current research trends in electrical discharge machining (EDM). *Int J Machine Tools Manufacture* **2007**, *47* (7-8), 1214-1228. <https://doi.org/10.1016/j.ijmachtools.2006.08.026>.
10. Ekmekci, B. Residual stresses and white layer in electric discharge machining (EDM). *Appl Surface Sci* **2007**, *253*, 9234–9240. <https://doi.org/10.1016/j.apsusc.2007.05.078>.
11. Ho, C.-C.; Chang, Y.-J.; Hsu, J.-C.; Kuo, C.-L.; Huang, Fu-C. Experimental Investigation of Thermal Strain Caused by Electrical Discharge Machining on Stainless Steel SUS430. *Sens Mater* **2017**, *29* (11), 1615–1623. <http://dx.doi.org/10.18494/SAM.2017.1735>.
12. Żyra, A.; Bogucki R.; Podolak-Lejtas A.; Skoczypiec, S. Research on influence of heat treatment scheme of Ti10V2Fe3Al alloy on technological surface integrity after electrodischarge machining. *J Manufacturing Proc* **2021**, *62*, 47-57. <https://doi.org/10.1016/j.jmapro.2020.12.038>.
13. Moritz, S.; Schmidt, A.; Sann, J.; Thoma, M.H. Surface modifications caused by cold atmospheric plasma sterilization treatment. *J. Phys. D: Appl. Phys.* **2020**, *53*, 325203. <https://doi.org/10.1088/1361-6463/ab88e9>.
14. Cakil, T.; Carlak, H.F.; Ozen, S. The Indirect Effect of Lightning Electromagnetic Pulses on Electrostatic, Electromagnetic Fields and Induced Voltages in Overhead Energy Transmission Lines. *Appl Sci* **2024**, *14*, 3090. <https://doi.org/10.3390/app14073090>.
15. Piskarev, I.M.; Aristova, N.A.; Ivanova, I.P. Comparison of mechanisms for the action of cold electric discharge plasma and hot pulsed discharge plasma emission on water solutions. *J Phys: Conf Ser* **2021**, *2055*, 012011. <https://doi.org/10.1088/1742-6596/2055/1/012011>.
16. Piskarev, I.M.; Ivanova, I.P. Comparison of Chemistry Induced by Direct and Indirect Plasma Treatment of Water to the Effect of UV Radiation. *Plasma Chem Plasma Process* **2021**, *41*, 447–475. <https://doi.org/10.1007/s11090-020-10127-6>.
17. Dirks, T, Yayci, A.; Klopsch, S.; et al. Immobilization protects enzymes from plasma-mediated inactivation. *J. R. Soc. Interface* **2023**, *20*, 20230299. <https://doi.org/10.1098/rsif.2023.0299>.
18. Zhou, C.; Hu, Y.; Zhou, Y.; Yu, H. et al. Air and argon cold plasma effects on lipolytic enzymes inactivation, physicochemical properties and volatile profiles of lightly-milled rice. *Food Chem* **2024**, *445*, 138699. <https://doi.org/10.1016/j.foodchem.2024.138699>.
19. Ivanov, Y.; Frantsuzov, P.; Zöllner, A. et al. Atomic Force Microscopy Study of Protein–Protein Interactions in the Cytochrome CYP11A1 (P450scc)-Containing Steroid Hydroxylase System. *Nanoscale Res Lett* **2011**, *6*, 54. <https://doi.org/10.1007/s11671-010-9809-5>.

20. Ivanov, Y.D.; Bukharina, N.S.; Shumov, I.D. et al. AFM-Based Monitoring of Enzymatic Activity of Individual Molecules of Cytochrome CYP102A1. *Biosensors*, **2025**, *15* (5), 303. <https://doi.org/10.3390/bios15050303>.
21. Sun, J.; Sun, F.; Xu, B.; Gu, N. The quasi-one-dimensional assembly of horseradish peroxidase molecules in presence of the alternating magnetic field. *Coll Surf A: Physicochem. Eng. Aspects* **2010**, *360*, 94–98. <https://doi.org/10.1016/j.colsurfa.2010.02.012>.
22. Sun, J.; Zhou, H.; Jin, Y.; Wang, M.; Gu, N. Magnetically enhanced dielectrophoretic assembly of horseradish peroxidase molecules: Chaining and molecular monolayers. *ChemPhysChem* **2008**, *9*, 1847–1850. <https://doi.org/10.1002/cphc.200800237>.
23. Ivanov, Y.D.; Pleshakova, T.O.; Shumov, I.D. et al. AFM Imaging of Protein Aggregation in Studying the Impact of Knotted Electromagnetic Field on A Peroxidase. *Sci Rep* **2020**, *10*, 9022. <https://doi.org/10.1038/s41598-020-65888-z>.
24. Ivanov, Y.D.; Tatur, V.Y.; Pleshakova, T.O. et al. Effect of Spherical Elements of Biosensors and Bioreactors on the Physicochemical Properties of a Peroxidase Protein. *Polymers* **2021**, *13* (10), 1601. <https://doi.org/10.3390/polym13101601>.
25. Eberhart, M.E.; Wilson, T.R.; Jones, T.E.; Alexandrova, A.N. Electric fields imbue enzyme reactivity by aligning active site fragment orbitals. *Proc Natl Acad Sci USA* **2024**, *121*(44), e2411976121. <https://doi.org/10.1073/pnas.2411976121>.
26. Archakov, A.I.; Bachmanova, G.P. *Cytochrome P450 and Active Oxygen*. Taylor & Francis, London, New-York, Philadelphia; 1990.
27. Neeli, R.; Girvan, H.M.; Lawrence, A. et al. The dimeric form of flavocytochrome P450 BM3 is catalytically functional as a fatty acid hydroxylase. *FEBS Lett* **2005**, *579*, 5582–5588. <https://doi.org/10.1016/j.febslet.2005.09.023>.
28. Khmelevtsova, L.E.; Sazykin, I.S.; Azhogina, T.N. et al. Prokaryotic Peroxidases and Their Application in Biotechnology (Review). *Appl Biochem Microbiol* **2020**, *56*, 373–380. <https://doi.org/10.1134/S0003683820030059>.
29. Ziborov, V.S.; Pleshakova, T.O.; Shumov, I.D. et al. The Impact of Fast-Rise-Time Electromagnetic Field and Pressure on the Aggregation of Peroxidase upon Its Adsorption onto Mica. *Appl Sci* **2021**, *11* (24), 11677. <https://doi.org/10.3390/app112411677>.
30. Davydov, D.R.; Hui, Bon Hoa, G.; Peterson, J.A. Dynamics of protein-bound water in the heme domain of P450BM3 studied by high-pressure spectroscopy: Comparison with P450cam and P450 2B4. *Biochemistry* **1999**, *38*, 751–761. <https://doi.org/10.1021/bi981397a>.
31. Yao, Y.; Zhang, B.; Pang, Y. et al. The effect of radio frequency heating on the inactivation and structure of horseradish peroxidase. *Food Chem* **2023**, *398*, 133875. <https://doi.org/10.1016/j.foodchem.2022.133875>.
32. Emamdadi, N.; Gholizadeh, M.; Housaindokht, M.R. Investigation of static magnetic field effect on horseradish peroxidase enzyme activity and stability in enzymatic oxidation process. *Int J Biol Macromolecules* **2021**, *170*, 189–195. <https://doi.org/10.1016/j.ijbiomac.2020.12.034>.
33. Kodera, N.; Yamamoto, D.; Ishikawa, R. et al. Video imaging of walking myosin V by high-speed atomic force microscopy. *Nature* **2010**, *468*, 72–76. <https://doi.org/10.1038/nature09450>.
34. Ando, T.; Uchihashi, T. & Scheuring, S. Filming biomolecular processes by high-speed atomic force microscopy. *Chem Rev* **2014**, *114*, 3120–3188. <https://doi.org/10.1021/cr4003837>.
35. Takeda, K.; Uchihashi, T.; Watanabe, H. et al. Real-Time Dynamic Adsorption Processes of Cytochrome c on an Electrode Observed through Electrochemical High-Speed Atomic Force Microscopy. *PLoS ONE* **2015**, *10*(2), e0116685. <https://doi.org/10.1371/journal.pone.0116685>.
36. Sato, K.; Kanaoka, Y.; Tsukazaki, T.; Uchihashi, T.; Mori, T. Estimating Protein Conformational States from High-Speed AFM Images with Molecular Dynamics and Deep Learning. *J Chem Inf Model* **2026**, XXXX(XXX), XXX-XXX. <https://doi.org/10.1021/acs.jcim.6c00142>.
37. Dus, K.; Katagiri, M.; Yu, C.-A.; Erbes, D.L.; Gunsalus, I.C. Chemical Characterization of Cytochrome P-450cam\*. *Biochem Biophys Res Commun* **1970**, *40*(6), 1423–1430. [https://doi.org/10.1016/0006-291X\(70\)90026-4](https://doi.org/10.1016/0006-291X(70)90026-4).

38. Valikhani, D.; Bolivar, J.M.; Pelletier, J.N. An Overview of Cytochrome P450 Immobilization Strategies for Drug Metabolism Studies, Biosensing, and Biocatalytic Applications: Challenges and Opportunities. *ACS Catal* **2021**, *11*, 9418–9434. <https://doi.org/10.1021/acscatal.1c02017>.
39. Bisson, L. F.; Thorner, J. Thymidylate Synthetase from *Saccharomyces cerevisiae*. *J Biol Chem* **1981**, *256*(23), 12456–12462. [https://doi.org/10.1016/S0021-9258\(18\)43295-4](https://doi.org/10.1016/S0021-9258(18)43295-4).
40. Mori, Q.; Imae, T. AFM investigation of the adsorption process of bovine serum albumin on mica. *Coll Surf B: Biointerfaces* **1997**, *9*, 31–36. [https://doi.org/10.1016/S0927-7765\(97\)00005-2](https://doi.org/10.1016/S0927-7765(97)00005-2).
41. Andrade, J.D.; Hlady, V.; Wei, A.P. Adsorption of complex proteins at interfaces. *Pure & Appl Chem*. **1992**, *64*(11), 1777–1781. <https://doi.org/10.1351/pac199264111777>.
42. Luo, Q.; Andrade, J.D. Cooperative Adsorption of Proteins onto Hydroxyapatite. *J Coll Interface Sci* **1998**, *200*, 104–113. <https://doi.org/10.1006/jcis.1997.5364>.
43. Kim, D.T.; Blanch, H.W.; Radke, C.J. Direct Imaging of Lysozyme Adsorption onto Mica by Atomic Force Microscopy. *Langmuir* **2002**, *18*, 5841–5850. <https://doi.org/10.1021/la0256331>.
44. Welinder, K.G. Amino Acid Sequence Studies of Horseradish Peroxidase. Amino and Carboxyl Termini, Cyanogen Bromide and Tryptic Fragments, the Complete Sequence, and Some Structural Characteristics of Horseradish Peroxidase C. *Eur J Biochem* **1979**, *96*, 483–502. <https://doi.org/10.1111/j.1432-1033.1979.tb13061.x>.
45. Amano, H, Yusa, N, Nozawa, T. Effect of residual stress on the electromagnetic non-destructive testing signals from components made of F82H steel. *Fusion Eng Design* **2025**, *217*, 115177. <https://doi.org/10.1016/j.fusengdes.2025.115177>.
46. Gauthier, J.; Krause T.W.; Atherton, D.L. Measurement of residual stress in steel using the magnetic Barkhausen noise technique. *NDT & E Int* **1998**, *31* (1), 23–31. [https://doi.org/10.1016/S0963-8695\(97\)00023-6](https://doi.org/10.1016/S0963-8695(97)00023-6).
47. Qin, R, Su, S. Thermodynamics of crack healing under electropulsing. *J Mater Res* **2002**, *17* (8), 2048–2052. <https://doi.org/10.1557/JMR.2002.0303>.
48. Song, Y.; Wu, W.; Yu, Y. et al. Effects of Electric and Magnetic Treatments on Microstructures of Solid Metals: A Review. *Chin J Mech Eng* **2023**, *36*, 139. <https://doi.org/10.1186/s10033-023-00961-y>.
49. Lee W.; Gheorghie A.H.; Tiurev K.; Ollikainen T.; Möttönen M.; Hall, D.S. Synthetic electromagnetic knot in a three-dimensional skyrmion. *Sci Adv* **2018**, *4* (3), eaao3820. <https://doi.org/10.1126/sciadv.aao3820>.
50. Nefedov, E. I.; Ermolaev, Y. M., Smelov, M. V. Experimental study of excitation and propagation of nodular electromagnetic waves in various media. *Radio Eng* **2014**, *2*, 31–34.
51. Vitagliano, L.; Berisio, R.; De Simone, A. Role of Hydration in Collagen Recognition by Bacterial Adhesins. *Biophys J*. **2011**, *100* (9), 2253–226. <https://doi.org/10.1016/j.bpj.2011.03.033>.
52. Beaufilet, C.; Man, H.-M.; de Poulpique, A.; Mazurenko, I.; Lojou, E. From Enzyme Stability to Enzymatic Bioelectrode Stabilization Processes. *Catalysts* **2021**, *11* (4), 497. <https://doi.org/10.3390/catal11040497>.
53. Krainer, F.W.; Glieder, A. An updated view on horseradish peroxidases: recombinant production and biotechnological applications. *Appl Microbiol Biotechnol* **2015**, *99*, 1611–1625. <https://doi.org/10.1007/s00253-014-6346-7>.
54. Rani, D.; Pachauri, V.; Madaboosi, N. et al. Top-Down Fabricated Silicon Nanowire Arrays for Field-Effect Detection of Prostate-Specific Antigen. *ACS Omega* **2018**, *3*, 8471–8482. <https://doi.org/10.1021/acsomega.8b00990>.
55. Stern, E.; Klemic, J.; Routenberg, D. et al. Label-free immunodetection with CMOS-compatible semiconducting nanowires. *Nature* **2007**, *445*, 519–522. <https://doi.org/10.1038/nature05498>.
56. Stern, E.; Vacic, A.; Rajan, N. et al. Label-free biomarker detection from whole blood. *Nature Nanotech* **2010**, *5*, 138–142. <https://doi.org/10.1038/nnano.2009.353>.
57. Elfström N.; Juhasz R.; Sychugov I.; Engfeldt T.; Eriksson Karlström A.; Linnros J. Surface Charge Sensitivity of Silicon Nanowires: Size Dependence. *Nano Lett* **2007**, *7*(9), 2608–2612. <https://doi.org/10.1021/nl0709017>.
58. Kiselyova, O.I.; Yaminsky, I.V.; Ivanov, Yu.D. et al. AFM study of membrane proteins, cytochrome P450 2B4, and NADPH–Cytochrome P450 reductase and their complex formation. *Arch Biochem Biophys* **1999**, *371*(1), 1–7. <https://doi.org/10.1006/abbi.1999.1412>.

59. Sanders, S.A.; Bray, R.C.; Smith, A.T. pH-Dependent properties of a mutant horseradish peroxidase isoenzyme C in which Arg38 has been replaced with lysine. *Eur J Biochem* **1994**, *224*(3), 1029–1037. <https://doi.org/10.1111/j.1432-1033.1994.01029.x>.
60. Ivanov, Y.D.; Tatur, V.Y.; Shumov, I.D. et al. The Effect of a Dodecahedron-Shaped Structure on the Properties of an Enzyme. *J Funct Biomater* **2022**, *13*, 166. <https://doi.org/10.3390/jfb13040166>.

**Disclaimer/Publisher's Note:** The statements, opinions and data contained in all publications are solely those of the individual author(s) and contributor(s) and not of MDPI and/or the editor(s). MDPI and/or the editor(s) disclaim responsibility for any injury to people or property resulting from any ideas, methods, instructions or products referred to in the content.